IEEE Access
Multidisciplinary | Rapid Review | Open Access Journal

Received December 19, 2019, accepted January 3, 2020, date of publication January 10, 2020, date of current version January 22, 2020.

Digital Object Identifier 10.1109/ACCESS.2020.2965652

Symmetrical/Asymmetrical Winding Reconfiguration in Multiphase Machines

MARKO SLUNJSKI, (Student Member, IEEE), OBRAD DORDEVIC, (Member, IEEE), MARTIN JONES, AND EMIL LEVI, (Fellow, IEEE)
Faculty of Engineering and Technology, Liverpool John Moores University, Liverpool L3 3AF, U.K.
Corresponding author: Emil Levi (e.levi@ljmu.ac.uk)

ABSTRACT This paper investigates multiphase drives in which winding configuration (symmetrical or asymmetrical) can be easily obtained by only rearranging voltage source inverter (VSI) power supply cables at the machine's terminal box. The type of the machines where this is possible is identified and the examples of reconfiguration are given and explained. Following from the examples (for nine- and fifteen-phase cases), a general reconfiguration algorithm is introduced. As shown, changing asymmetrical to symmetrical winding configuration (and vice versa) means that just another mimic diagram needs to be placed over the existing one on the machine's terminal box. Possible reconfigurations of a six-phase machine, which do not follow the same pattern, are also addressed. Differences caused by different winding configuration are identified and experimentally confirmed using a nine-phase surface mounted permanent magnet synchronous machine (PMSM) and a nine-phase induction machine (IM).

INDEX TERMS Multiphase drives, symmetrical/asymmetrical winding reconfiguration, PMSM, induction machine, harmonic mapping.

I. INTRODUCTION

The advantages of multiphase machines over their three-phase counterparts are nowadays well understood [1]–[3] and have led to their use in various transportation applications (e.g. high-speed elevators, more-electric planes, trains, ship propulsion [2]), as well as in power generation systems (for example, wind turbines) [2].

With regard to the number of phases, multiphase machines with composite numbers of phases (such as, for example, those composed of multiple three-phase sets) can be considered as a special category. Such machines are the most popular multiphase machines in real-world industrial applications since they provide modularity and their control is also relatively easily related to the control of a three-phase machine.

For multiphase machines with a composite number of phases two main modelling approaches and hence transformations are predominantly used: multiple *d-q* (also known as multi-stator approach) and vector space decomposition (VSD) transformation [4], [5]. Despite the disadvantages when compared to the VSD [4], multi-stator method is a commonly used approach in industry because it uses well-known three-phase machine technologies (i.e. independent control over each individual, three-phase, winding set). On the other hand, the use of a proper VSD transformation will not only decouple the machine into flux/torque producing (α-β) and non-producing (x-y) components, but will also uniquely map odd-order harmonics in the subspaces [1], [2].

Form of the VSD transformation matrix for an n-phase machine with a composite number of phases depends on the number of isolated neutral points and on the phase propagation angle between machine's winding sets. The sets can be arranged as symmetrical if spatial shift between any two consecutive phase windings is $2\pi/n$ or asymmetrical if spatial shift between the corresponding phases of the winding sets is π/n (where n stands for the number of stator phases). Different ways of obtaining VSD matrices have been devised in [6], [7] where nine-phase asymmetrical synchronous machine model has been decomposed into orthogonal subspaces.

A general (n-phase) algorithm for VSD matrix transformation development, applicable to any symmetrical or asymmetrical configuration with single or multiple isolated neutral points, was presented in [8], where arbitrary power sharing among three-phase winding sets was tested on a nine-phase asymmetrical induction generator with indirect rotor

The associate editor coordinating the review of this manuscript and approving it for publication was Christopher H. T. Lee.

field-oriented control (FOC). Regarding cases where symmetrical nine-phase machines have been in the focus for different applications, the following is a brief summary. Symmetrical induction machine was investigated in [9] for torque improvement using third harmonic current injection, while for the same purpose, a symmetrical interior PMSM machine was used in [10]. In [11], a symmetrical nine-phase machine was tested for high-speed elevator control, while design and optimization of a symmetrical nine-phase flux-switching PM generator for wind power systems was investigated in [12].

Asymmetrical and symmetrical configurations are rarely treated together for the same phase number, primarily since for each particular case it is known which topology is better. A rare exception is [13], where, to test derived symmetrical/asymmetrical structure control algorithms, two different six-phase induction machines (with different parameters and windings) were used.

In this work, a method for simple winding reconfiguration is presented. If the machine is with a composite odd phase number (e.g. nine-, fifteen-, etc.), winding configuration can be easily changed by only VSI power leads rearrangement in the machine's terminal box. Such a possibility was briefly mentioned in [14] and restated in [11], but has never been explained in detail, generalised or experimentally verified. It therefore appears that this knowledge, common to electric machine designers, has so far by and large escaped the attention of the drive control community. As it will be shown here, changing asymmetrical to symmetrical winding configuration (and vice versa) means that just another mimic diagram needs to be placed over the existing one on the machine's terminal box.

The paper is organised as follows. In Section II, a composite odd phase number group of machines, for which symmetrical/asymmetrical reconfiguration is possible, is defined. The theoretical considerations are demonstrated for nine- and fifteen-phase case. Based on those two examples, in Section III a general rearrangement algorithm is introduced. To study differences in machines with reconfigured windings, simulation and experimental results are presented in Section IV. Conclusions are given in Section V.

II. MULTIPHASE MACHINE WINDING ARRANGEMENTS AND CHANGE OF THE CONFIGURATION

Regardless of the type of the machine (synchronous or induction), multiphase machines can be classified into two distinct groups: machines with a prime number of phases and machines with an even number or a composite odd number of phases. If the machine is with a prime number of phases (i.e. 3, 5, 7, 11, ...), spatial displacement between any two consecutive phases is equal to $2\pi/n$ and there is a single isolated neutral point. On the other hand, machines with an even number or a composite odd number of phases (i.e. 6, 9, 12, ...) can be with k_{ws} winding sets, each having a phases, and can be with a single or k_{ws} isolated neutral points. If the winding sets are three-phase ones ($a = 3$), then the analysed machine is a multiple three-phase winding machine ($n = 3{\cdot}k_{ws}$). In many applications today, this is the preferable configuration because of similarities with the well-known three-phase machine topologies.

The stator of a multiphase machine is arranged either in symmetrical or asymmetrical winding configuration, i.e. with spatial displacement between consecutive phases equal to $2\pi/n$ or π/n, respectively. Nevertheless, machines where both winding configurations (symmetrical and asymmetrical) can be easily achieved by only rearranging the supply cables at the machine terminal box also exist. For these machines, change of the winding configuration can be accomplished only if both (the start and the end) winding terminals are accessible for all phases; this winding type is known as open-ended. Multiphase machines used in research laboratories are usually with open-end winding because they are custom-made and commonly all $2 \cdot n$ winding terminals are available in the machine's terminal box. In other words, the neutral point(s) of the machine are left to be formed according to the user requirements.

A. IDENTIFICATION OF THE MACHINES FOR WHICH REARRANGEMENT IS POSSIBLE

The reconfigurations that lead from symmetrical (phase shift between phases equal $2\pi/n$) to asymmetrical configuration (phase shift between consecutive sets equal π/n), and vice versa, are, as the main objective of this work, analysed first. Reconfigurations that lead to double-winding configurations (with 0° phase shift between the winding sets) are special reconfiguration cases and as such are discussed at the end of Section II.B.

Changing asymmetrical winding configuration to symmetrical and vice versa by only rearranging VSI supply leads in the machine's terminal box (and reconfiguring neutral point(s) connections) is possible only when the number of phases is a composite odd number equal to or higher than 9. Also, both the number of phases per set a and the number of winding sets k_{ws} must be odd numbers equal to or higher than 3. The number of isolated neutral points is not relevant and the machine can be with single or multiple (k_{ws}) isolated neutral points. Mathematical expression for stated principle can be defined with:

$$n \geq 9; \quad k_{ws} = 3, 5, 7 \ldots; \; a = 3, 5, 7 \ldots \tag{1}$$

Based on the rule defined with (1), multiphase machines for which proposed reconfiguration is possible are given in Table 1. It must be noted that although mathematically correct, some of these configurations are not practical and are shown here just for the generalisation purpose.

Before the algorithm for reconfiguration is derived, labelling system for winding sets and corresponding phases in them must be defined. As already stated, analysed machines are with $n = a \cdot k_{ws}$, $n \geq 9$ number of phases. Winding sets are denoted with 1, 2, 3, ..., k_{ws} and each winding set can have a phases denoted with a, b, c, ... (e.g. $a1$ represents the first phase in the first set, $a2$ represents the first phase in the second set, etc.). Labelling always starts from phase

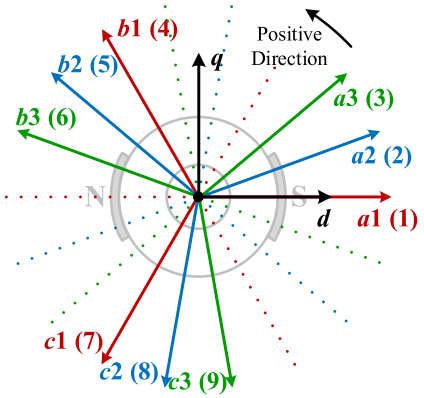

FIGURE 1. Example of a magnetic axis diagram for a nine-phase asymmetrical winding configuration.

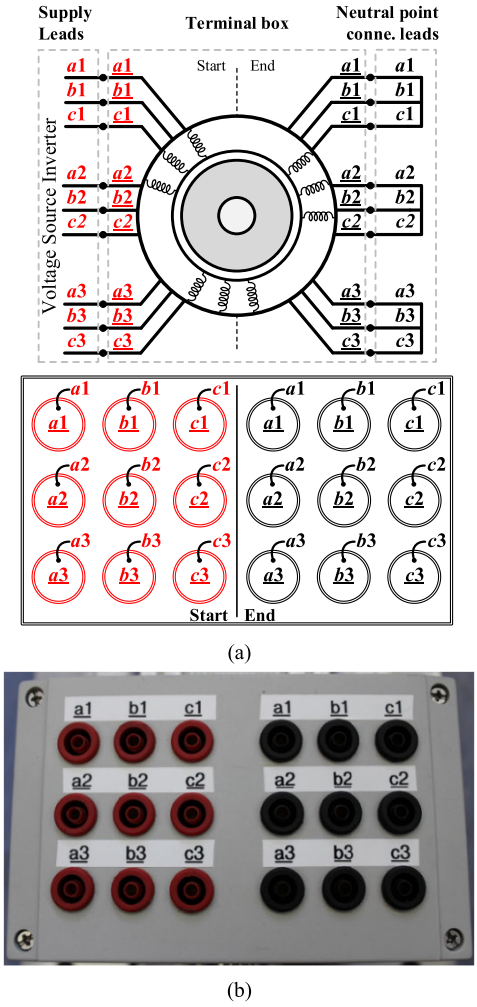

FIGURE 2. Example of a nine-phase (asymmetrical) winding with associated labelling: (a) nine-phase VSI power supply leads and the machine terminal box, and (b) terminal box mounted on the real machine.

$a1$ in Set-1, which is assumed to be placed at 0° angle. For a nine-phase machine, stated phase annotation can be seen in Fig. 1 (rotor configuration corresponds to the machine

TABLE 1. Machine configurations for which symmetrical/asymmetrical reconfiguration is possible.

$n \geq 9$	$k_{ws} = 3$	$k_{ws} = 5$	$k_{ws} = 7$	$k_{ws} = 9$	...
$a = 3$	9	15	21	27	...
$a = 5$	15	25	35	45	...
$a = 7$	21	35	49	63	...
$a = 9$	27	45	63	81	...
...	...	...	...	...	...

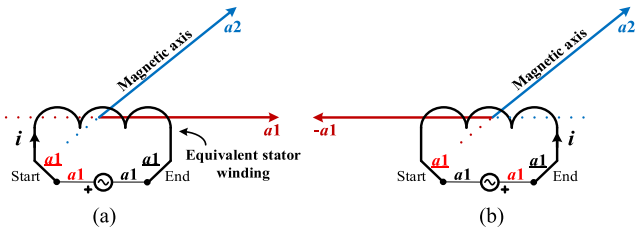

FIGURE 3. Representation of magnetic axis inversion after rearrangement of power supply leads in phase $a1$.

used in Section IV), where magnetic axes for asymmetrical configuration are shown. In addition to the phase labels ($a1$, $a2$, $a3$, etc.), phase sequential numbers ($1, 2, 3, \ldots, n$) are also shown in Fig. 1. They will play an important role in definition of the general symmetrical/asymmetrical reconfiguration algorithm.

In Fig. 2a, a nine-phase voltage source inverter power supply leads and neutral point(s) connection leads (upper plot) and open-end winding machine terminal box (bottom plot) are shown. As can be seen, both start and end terminals of the machine's windings are accessible ($2{\cdot}n = 18$). Starting winding terminals of every phase in the machine's terminal box are denoted with red underlined labels ($\underline{a1}$, $\underline{a2}$, …, $\underline{c3}$), while corresponding end winding terminals are denoted with black underlined labels ($\underline{a1}$, $\underline{a2}$, …, $\underline{c3}$). Similarly, VSI power supply leads are labelled with red $a1$, $a2$, …, $c3$ labels, while the leads used to form the neutral point(s) are denoted with black $a1$, $a2$, …, $c3$ labels. As already explained, the number of isolated neutral points is irrelevant and can be one or k_{ws}.

For the time being, three neutral points are assumed and arranged as shown in Fig. 2a. In Fig. 2b, terminal box mounted on a real nine-phase machines, used in experimental investigation, is shown.

B. CHANGE OF A WINDING CONFIGURATION BY REARRANGEMENT OF VSI POWER SUPPLY LEADS IN THE MACHINE'S TERMINAL BOX

From Fig. 1 one can see that if the magnetic axes of the second set (in blue) are rotated by 180°, i.e. inverted, a symmetrical machine configuration would be obtained. Therefore, the meaning of magnetic axis inversion should be explained first. This will be explained on inversion of the magnetic axis $a1$, as depicted in Fig. 3. In Fig. 3a the positive end of the inverter cable is connected to the start, red terminal, of the winding (while the end of the winding, black terminal,

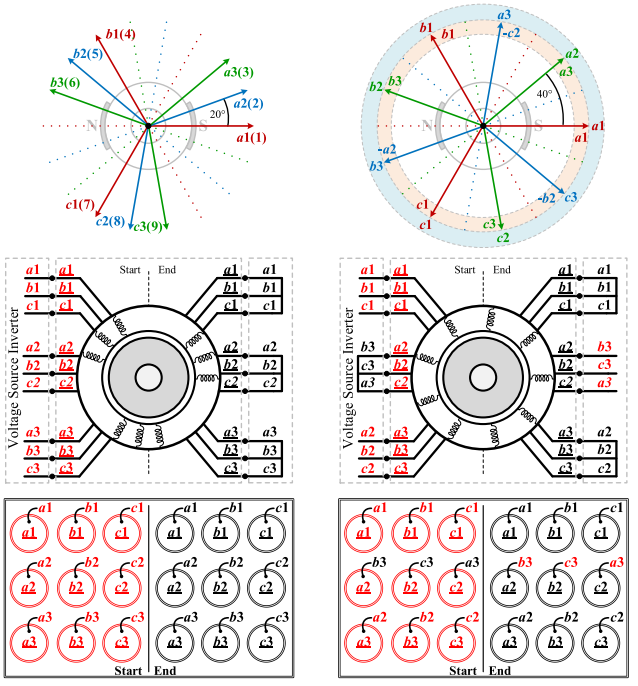

FIGURE 4. Asymmetrical to symmetrical winding reconfiguration: magnetic axis diagram (upper), VSI power supply leads rearrangement at the machine's terminal box (middle), and old and new mimic diagram (bottom plots).

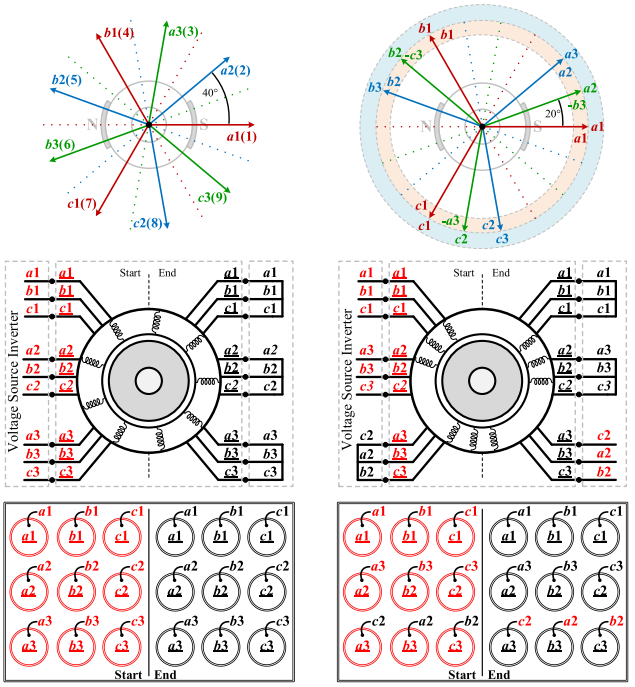

FIGURE 5. Symmetrical to asymmetrical winding reconfiguration: magnetic axis diagram (upper), VSI power supply leads rearrangement in the machine's terminal box (middle), and old and new mimic diagrams (bottom plots).

is forming a neutral point). This results in magnetic axis orientation as shown in Fig. 3a (red line; $a1$). If the voltage source power supply leads are rearranged as shown in Fig. 3b (if they are swapped), then new resulting magnetic axis is now oriented in the opposite direction ($-a1$).

By observing the whole set for which the inversion should be done (in this case the second set), this means that the neutral point connection of this set should be reallocated from black to the red side, and the supply leads should be connected to the black terminals. In this way the magnetic axes of the second set (initially located at 20°, 140° and 260°, Fig. 1), will be at 200°, 320° and 80°, respectively. For proper operation of the machine, phase delay of the reference for each phase must match with its magnetic axis angle. Only in this case, magnetic fluxes created by each set will be mutually aligned and will rotate together in the same direction. From Fig. 3, it may appear that software inversion, i.e. a multiplication of the reference by -1 for that phase, can have the same effect as the described hardware inversion. However, this would only mean that the initial position of the flux is changed for 180°. If all three sets are observed, and if the references of only one set are multiplied by -1, the flux generated by this set would not be aligned with the fluxes generated by the other two sets any more. This would result in a different current magnitude generated in that set. Hence, inversion of magnetic axes has to be done in hardware by moving the neutral point to the other side of the winding terminals.

An example of a machine with nine phases, i.e. with the number of phase sets $k_{ws} = 3$ ($a = 3$), is shown in Fig. 4. This figure illustrates how asymmetrical nine-phase machine can be easily reconfigured to be symmetrical. As already mentioned and as it is clear from Fig. 4, the first (and every following odd number) winding set (Set-1, Set-3) should stay at the same angular position. Note that this is true for any other meaningful configurations even if $n > 9$. The second winding set, Set-2 (or in general case every even numbered set), must be inverted. In the shown case, start and end supply leads are swapped for the phases $a2$, $b2$, $c2$, i.e. rotational shift of magnetic axes for 180° is performed. In accordance with the labelling system, Set-2 of original asymmetrical configuration becomes Set-3, and Set-3 becomes Set-2 of the symmetrical configuration. Hence, the labels should be changed as indicated in Fig. 4 (upper plot, blue and red circle). Obtained new winding arrangement is with 40° spatial displacement between consecutive phases, which indeed represents symmetrical nine-phase machine ($2\pi/n$). How to rearrange VSI supply leads at the terminal box to perform this reconfiguration is shown Fig. 4, middle plots. Corresponding terminal boxes (mimic diagrams) are presented in Fig. 4, bottom plots. Therefore, if the original machine is with asymmetrical configuration and symmetrical is needed, new mimic diagram should be placed over the old one and the power supply leads must be arranged in accordance with the new mimic diagram.

The opposite case, how to change symmetrical configuration to asymmetrical, is shown in Fig. 5. In this case, the whole winding sets which contain phases numerated with the following numbers:

$$m = \frac{n+1+i}{2} \tag{2}$$

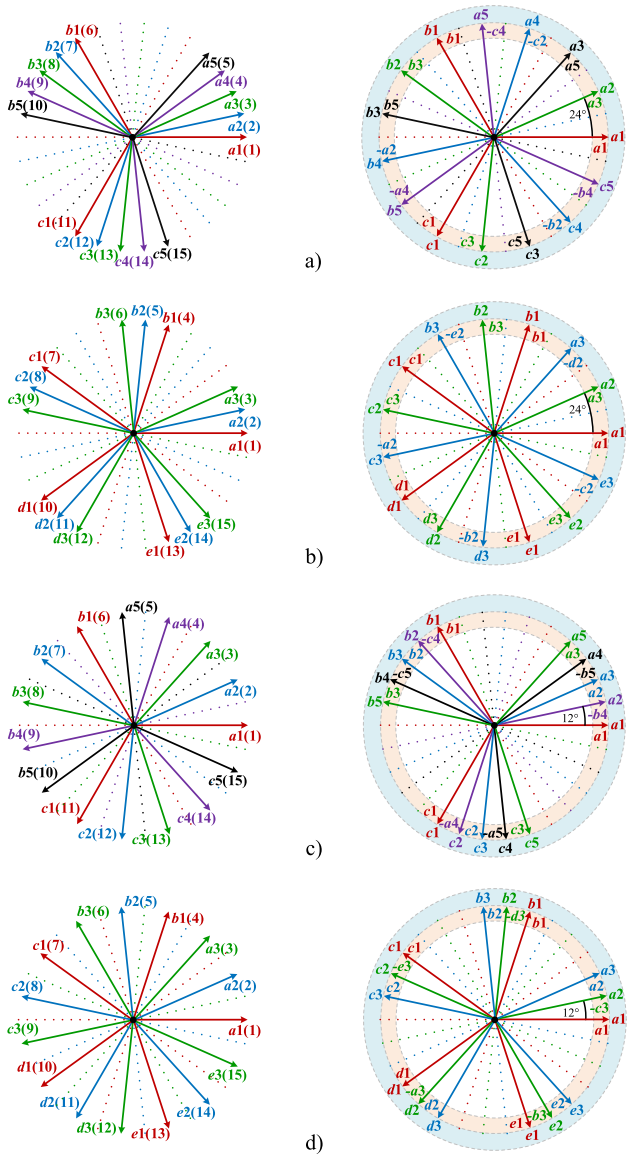

FIGURE 6. Winding reconfiguration in fifteen-phase machine. Asymmetrical to symmetrical for: (a) $k_{ws} = 5$, a = 3, (b) $k_{ws} = 3$, a = 5. Symmetrical to asymmetrical for: (c) $k_{ws} = 5$, a = 3, (d) $k_{ws} = 3$, a = 5.

should be inverted. In (2), i represents an integer even number smaller than or equal to the number of phase sets:

$$i = 2, 4, 6 \ldots \leq k_{ws} - 1 \tag{3}$$

For example, in nine-phase case ($k_{ws} = 3$), after applying (2)-(3), it is calculated that $i = 2$ and $m = 6$. The winding set which contains phase number 6 must be inverted. If phase diagram is observed, it is easy to conclude that this phase is in Set-3. Every phase in this set must now be inverted. By doing so, new spatial displacement is π/n, which means that asymmetrical configuration is achieved (Fig. 5, upper plots). Supply lead rearrangement is similar to the one explained for asymmetrical to symmetrical reconfiguration and is given in Fig. 5, middle. Mimic diagrams are given in Fig. 5, bottom.

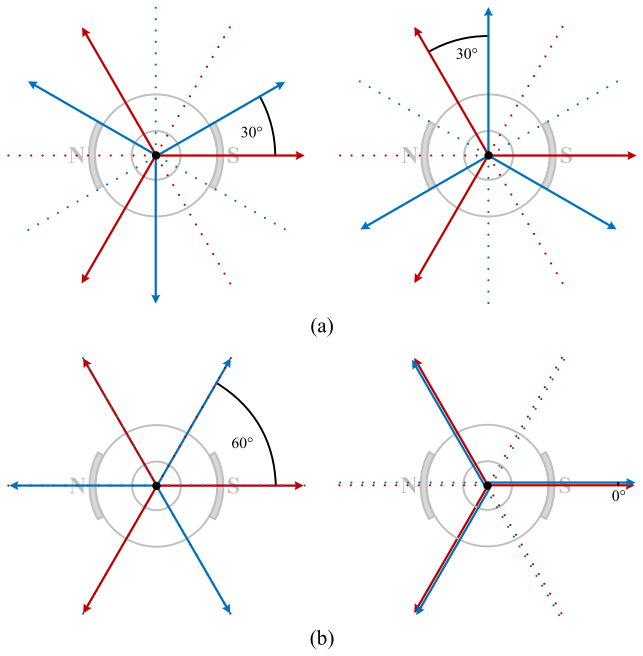

FIGURE 7. Winding reconfiguration in: (a) an asymmetrical, and (b) a symmetrical six-phase machine (blue set is inverted in both cases).

The same approach can be used for other configurations of Table 1. As an example, a simplified representation for fifteen-phase case is shown in Fig. 6. Fifteen-phase winding can be arranged in two different ways, with $k_{ws} = 5$, $a = 3$ or with $k_{ws} = 3$, $a = 5$. If the machine is asymmetrical with five three-phase winding sets ($k_{ws} = 5$), to achieve symmetrical configuration phases belonging to even sets (2nd and 4th) must be inverted. Following the same rule, if the fifteen-phase machine is with three-five-phase winding sets ($k_{ws} = 3$), the phases belonging to the 2nd set must be inverted. These cases are shown in Figs. 6a and b, respectively. As it can be seen from figures, in both cases new spatial displacement between consecutive phases is 24°.

To achieve asymmetrical winding configuration out of symmetrical fifteen-phase machine, two different possibilities are again available. If new required winding arrangement is with $k_{ws} = 5$, $a = 3$, using (2)-(3) it is easy to determine that the sets which contain phases numbered as 9 and 10 (i.e. Set-4 and Set-5) must be inverted. Following the same calculating principles, if winding arrangement is with $k_{ws} = 3$, $a = 5$, all phases in the set which contains phase number 9 (Set-4) must be inverted. Described rearrangements with new labels are shown in Figs. 6c and d, respectively. This time, new spatial displacement between consecutive winding sets is 12°.

As it can be concluded from Table 1, six-phase winding configuration is not in the group of the machines for which proposed reconfiguration can be achieved. Nevertheless, this is one of the most commonly used multiphase machine types; hence possible winding rearrangements are also briefly discussed here. Reconfiguration (that is, inversion of one

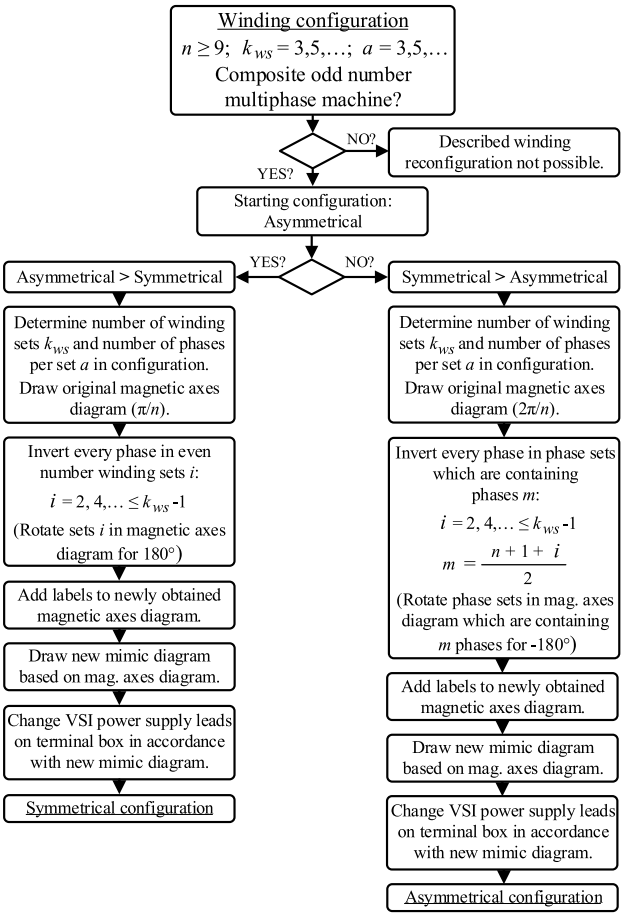

FIGURE 8. Flowchart diagram for machine winding reconfiguration.

three-phase set) in an asymmetrical six-phase machine will always result in another asymmetrical winding configuration, meaning that the winding type does not change (Fig. 7a). Therefore, for the asymmetrical six-phase case, the reconfiguration does not bring in anything new. On the other hand, reconfiguration of a symmetrical six-phase winding will result in a double-winding three-phase machine (with 0° shift between three-phase sets), as shown in Fig. 7b. The new configuration is obviously not asymmetrical (it is different from asymmetrical six-phase machines), but it can be useful in practice, e.g. [15]. Similarly, double-winding configuration can be also achieved in, for example, ten-phase symmetrical machine (new configuration is double-winding five-phase symmetrical), twelve-phase symmetrical machine (new configuration is double-winding six-phase asymmetrical), and so on.

III. GENERAL ALGORITHM FOR WINDING RECONFIGURATION

Having in mind (1)-(3) and the previous examples, a general algorithm for asymmetrical to symmetrical winding configuration change (and vice versa) can now be introduced (Fig. 8). Knowing the starting winding configuration, magnetic axis

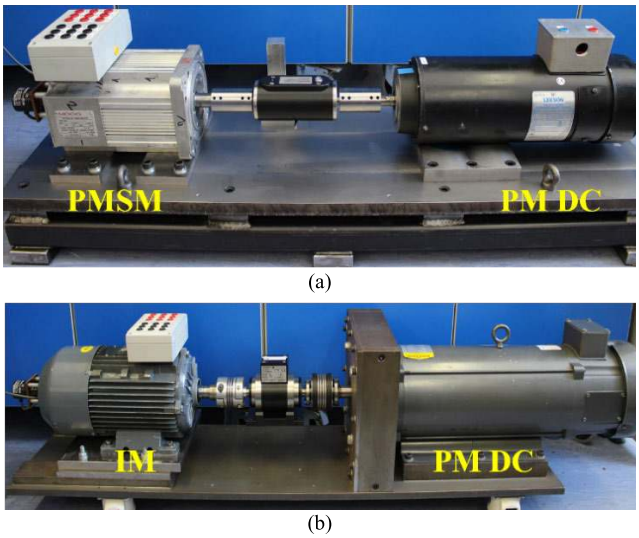

FIGURE 9. Nine-phase PMSM (a) and induction machine (b) experimental setups.

diagram can be drawn. If starting configuration of a multiphase machine (with composite odd number of phases) is asymmetrical, in order to convert it to symmetrical configuration, phases belonging to even sets must be rotated by 180°. Essentially, this means that for every phase in these sets start and end supply leads (start lead is coming from the inverter and end lead is forming the neutral point) in the terminal box should be swapped (Fig. 4). The labels should be changed according to the labelling system presented at the beginning of Section II-A. By doing so, spatial displacement between sequential phases in the new configuration is $2\pi/n$, which means that symmetrical configuration is achieved. If starting winding configuration is symmetrical, a similar rule can be applied. This time, it is important to note that to achieve asymmetrical configuration out of symmetrical, phases in winding sets with phase numbers m which are calculated using (2)-(3), must be inverted. An easy to follow diagram for both (re)configurations is presented in Fig. 8.

In real world applications, once when the phase number is selected, the preferred configuration (symmetrical or asymmetrical) is in essence known. In general, the required spacing between multiple winding sets for best performance is π/n for an even number of sets and $2\pi/n$ for an odd number of sets [5]. Nevertheless, as the multiphase machine prototypes for laboratories are commonly obtained by rewinding their three phase counterparts, one or the other configuration can be more suitable, depending on the envisaged research goal. Hence the practical importance of the described work relates primarily to the laboratory environment, where in most cases a single machine is available. Provided that the re-wound (multiphase) machine is with open end-windings, new control algorithms can be tested for both winding configurations using a single machine.

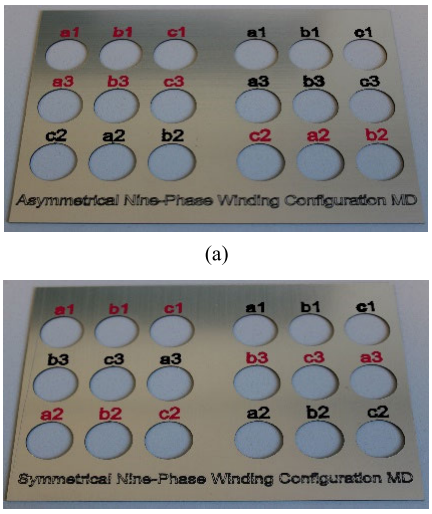

FIGURE 10. Mimic diagrams for a nine-phase winding reconfiguration: (a) symmetrical to asymmetrical and (b) asymmetrical to symmetrical.

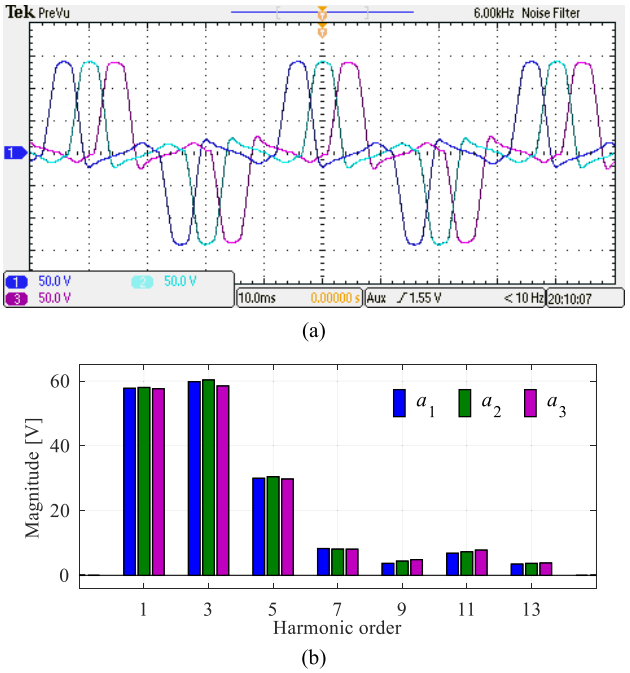

FIGURE 11. Back-EMF (phases *a*1, *a*2, *a*3) recorded experimentally in symmetrical nine-phase PMSM (a) and corresponding FFT (b).

IV. EXPERIMENTAL VALIDATION

To verify theoretical considerations, two experimental setups, based on a nine-phase PMSM investigated in [16] and on IM studied in [8], have been used (Figs. 9a and b, respectively). Both machines are with single pole-pair. Windings of the machines are changed and different performance validation tests were conducted. The shafts of the machines are coupled to the dc machines (used for loading) by a Datum Electronics M425 (for PMSM) and Magtrol TM250 (for IM) torque meters. The machines are supplied using two custom-made multiphase inverters (with up to 8 phases each) with common dc-link. Both inverters are based on Infineon FS50R12KE3 IGBT modules. The inverters have hardware-implemented dead time of 6 μs. Inverter dc-link voltage (450 V) is provided by Sorensen SGI600/25 single quadrant dc-voltage source. Measurement and control are realized by rapid prototyping platform dSPACE ds1006. An ADC board (ds2004) is used to acquire phase currents measured by the inverter's internal LEM sensors, while an incremental encoder board (ds3002) provides the speed/position from the optical encoder. Additional measurements are taken using Tektronix DPO/MSO 2014 oscilloscopes, equipped with current (Pico Technology TA189) and high-voltage differential (Tektronix P5205A) probes. Two mimic diagrams for nine-phase winding reconfiguration are also made (Fig. 10). Mimic diagrams show how supply leads should be rearranged, hence labels on them are not underlined. Original winding configuration of the PMSM is symmetrical (with a single isolated neutral point) while for the induction machine it is asymmetrical (with three isolated neutrals). Machines with such winding distribution were chosen so that winding reconfiguration in both directions can be tested on two different types of machines.

Nine-phase PMSM was first investigated in [16] for torque improvement purpose. Magnets on the two-pole rotor are shortened, which causes production of highly non-sinusoidal back-electromotive force (EMF) in the stator windings (Fig. 11a). FFT analysis of the EMF reveals a high-magnitude harmonic spectrum, with third harmonic's magnitude almost equal to the fundamental (Fig. 11b). As concluded in [16], if third harmonic current injection is employed in the control algorithm, output torque can be significantly improved. Injecting third harmonic current into stator currents to couple with back-EMF was possible because, as shown with corresponding equations next, the third harmonic stator currents in symmetrical nine-phase machine sum to zero:

$$
\begin{aligned}
&i_{sa1,3} = i_3\cos(3\omega t - 0); \quad i_{sb1,3} = i_3\cos(3\omega t - 0);\\
&i_{sc1,3} = i_3\cos(3\omega t - 0)\\
&i_{sa2,3} = i_3\cos(3\omega t - \frac{2\pi}{3}); \quad i_{sb2,3} = i_3\cos(3\omega t - \frac{2\pi}{3});\\
&i_{sc2,3} = i_3\cos(3\omega t - \frac{2\pi}{3})\\
&i_{sa3,3} = i_3\cos(3\omega t - \frac{4\pi}{3}); \quad i_{sb3,3} = i_3\cos(3\omega t - \frac{4\pi}{3});\\
&i_{sc3,3} = i_3\cos(3\omega t - \frac{4\pi}{3})\\
&\qquad \rightarrow \textit{Symmetrical Winding Distribution} \qquad (4)\\
&\qquad i_{sa1,3} + i_{sb1,3} + i_{sc1,3} + \ldots + i_{sc3,3} = 0 \qquad (5)
\end{aligned}
$$

The experimentally measured current waveforms are shown in Fig. 12. Four turns of wire were used for current measurement for higher precision (thus, $i_{abcn} = i_{osc}/4$). For the machine's control a simple FOC algorithm is implemented ($n_{\text{ref}} = 400$ rpm, $T_{\text{load}} \approx 1.1$ Nm). Fundamental current component is controlled for torque production, while

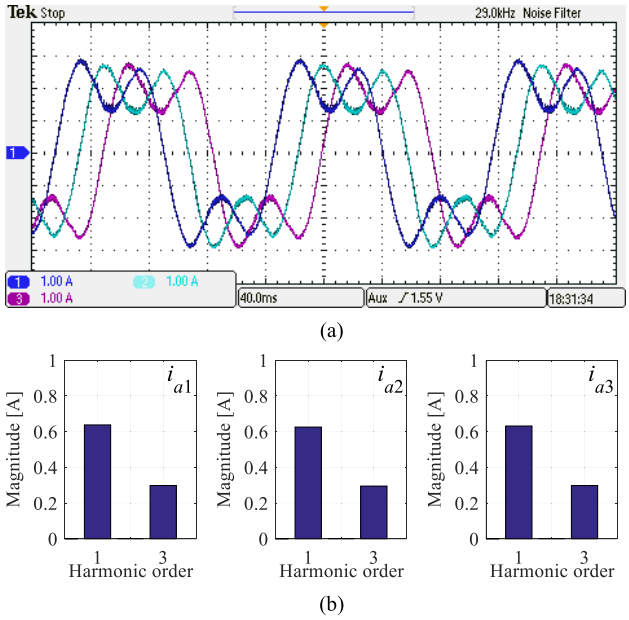

FIGURE 12. Symmetrical nine-phase machine: (a) phase currents (*a*1, *a*2, *a*3), and (b) corresponding FFTs.

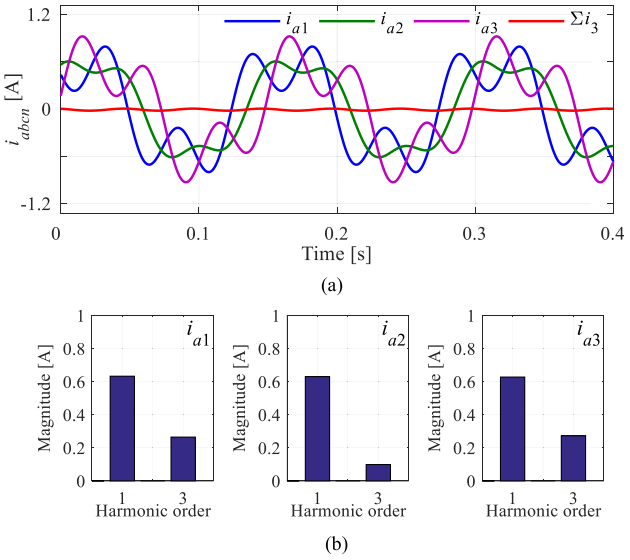

FIGURE 13. Asymmetrical nine-phase machine (simulation results): (a) phase currents (*a*1, *a*2, *a*3), and (b) corresponding FFTs.

the third current harmonic is not controlled (in essence, the third harmonic voltage generated by the PWM is zero on average in each switching period). In this way, the third EMF harmonic will induce the third harmonic in the current, which can then be analysed with respect to (4)-(5). As can be seen, in each winding set phase currents have the same shape (Fig. 12a), i.e. the stator third harmonic is equally distributed. Hence, (5) is obviously satisfied. Because only fundamental and the third harmonic component are considered and other induced current harmonics with order higher than 3 are not of interest here, FFT analysis (Fig. 12b) is shown only for these two harmonics. Induced harmonics with order higher than 3 are eliminated using vector proportional integral controllers, as described in [8].

On the other hand, current's third harmonic cannot have an equal distribution in an asymmetrical nine-phase machine. As it can be concluded from:

$$
\begin{aligned}
&i_{sa1,3} = i_3\cos(3\omega t - 0); \quad i_{sb1,3} = i_3\cos(3\omega t - 0);\\
&i_{sc1,3} = i_3\cos(3\omega t - 0)\\
&i_{sa2,3} = i_3\cos(3\omega t - \frac{\pi}{3}); \quad i_{sb2,3} = i_3\cos(3\omega t - \frac{\pi}{3});\\
&i_{sc2,3} = i_3\cos(3\omega t - \frac{\pi}{3})\\
&i_{sa3,3} = i_3\cos(3\omega t - \frac{2\pi}{3}); \quad i_{sb3,3} = i_3\cos(3\omega t - \frac{2\pi}{3});\\
&i_{sc3,3} = i_3\cos(3\omega t - \frac{2\pi}{3})\\
&\qquad \rightarrow \textit{Asymmetrical Winding Distribution} \qquad (6)\\
&i_{sa1,3} + i_{sb1,3} + i_{sc1,3} + \ldots + i_{sc3,3}\\
&\qquad = i_3(3\sin(3\omega t) - 3\sqrt{3}\cos(3\omega t)) \neq 0 \qquad (7)
\end{aligned}
$$

the third harmonic stator currents do not sum to zero.

To examine how the third harmonic phase current distribution will look like in an asymmetrical nine-phase PMSM, a simulation is performed first (applying the same control concept as in the symmetrical case). As illustrated in Fig. 13, the consequence of the inequality (7) is that the waveforms in the sets are obviously not of the same shape, i.e. the third harmonic currents attain different magnitudes in the different three-phase sets. Obtained different magnitudes of the third harmonics enable satisfaction of the condition $\Sigma i_3 = 0$ (red trace in Fig. 13a). To validate this experimentally, asymmetrical winding configuration was arranged in PMSM using mimic diagram from Fig. 10a. Recorded results are shown in Fig. 14. It is easy to conclude from the given results that different winding sets contain different amount of the corresponding harmonic component.

Comparison of simulation and experimental results in Figs. 13 and 14 confirms that the described reconfiguration procedure has successfully converted a symmetrical nine-phase machine into its asymmetrical counterpart. Small differences between the results are related to the standard simplifying assumptions used in the formulation of the simulation model (e.g. entirely equal phase windings). However, it should be noted that, because of the unequal current distribution, the third harmonic current injection is not a straightforward task for an asymmetrical nine-phase machine [17]. Hence, for control simplicity and in order to achieve higher torque using harmonic injection, symmetrical configuration of the machine is preferable [18]. In both [17] and [18], the same machine from [16] (Fig. 9a) was used. Reported torque improvement in [18] was $\approx 36\%$, while in [17] it was only around 15%.

Original winding configuration of the nine-phase induction machine (Fig. 9b) is asymmetrical. Parameter estimation tests were conducted first with the intention to obtain induction

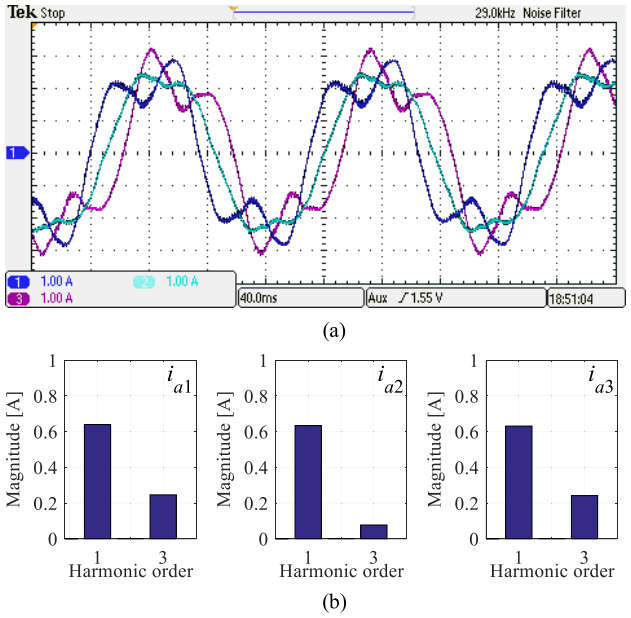

FIGURE 14. Asymmetrical nine-phase machine (experimental results): (a) phase currents ($a1$, $a2$, $a3$), and (b) corresponding FFTs.

TABLE 2. Asymmetrical IM parameters.

Parameter	Value
Stator resistance (R_s)	5.42 Ω
Rotor resistance (R_r)	1.88 Ω
Stator leakage inductance (L_{ls})	23.7 mH
Rotor leakage inductance (L_{lr})	11.2 mH
Mutual inductance (L_m)	968 mH

machine parameters for both configurations and to identify possible differences. To estimate parameters in both cases, well-known locked-rotor and no-load tests were used, similar as in [19]. A simple FOC was again applied.

Estimation was first performed for the original asymmetrical configuration to confirm the parameters reported in [8]. Obtained values are summarised in Table 2. By comparing these results with those in [8], a good agreement can be noted. Next, asymmetrical winding configuration was changed to symmetrical using mimic diagram from Fig. 10b and the same parameter estimation tests were repeated, with the results summarized in Table 3.

By comparing the results from Tables 2 and 3, it is easy to conclude that change of the machine's configuration did not cause any relevant changes in the electrical parameters (which is expected because, with the change of position of supply leads, no physical changes of the machine structure have been done). This means that, for a machine with reconfigured windings, the same FOC algorithm and the controller settings can be used (but of course with different phase shifts in decoupling transformation).

Because in closed-loop control machine electrical parameters are used for PI regulator tuning, the dynamics of the

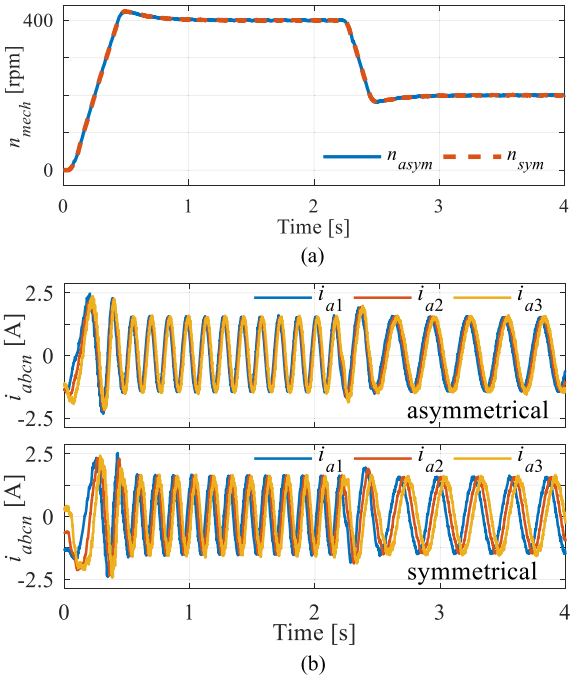

FIGURE 15. Experimentally recorded mechanical speed (a) and phase currents ($a1$, $a2$, $a3$) (b) under applied sequence for both winding configurations.

TABLE 3. Symmetrical IM parameters.

Parameter	Value
Stator resistance (R_s)	5.42 Ω
Rotor resistance (R_r)	1.84 Ω
Stator leakage inductance (L_{ls})	23.2 mH
Rotor leakage inductance (L_{lr})	10.9 mH
Mutual inductance (L_m)	987 mH

machine should not be different after reconfiguration. To validate this assumption, transient testing was performed experimentally, and corresponding results are given in Fig. 15. In both examined winding configurations speed was changed stepwise from 0 to 400 to 250 rpm and $T_{\text{load}} \approx 2$ Nm was kept constant. Based on the recorded results one can see that in both cases transient performance was the same (the same speed response, Fig. 15a). Also, after the reconfiguration, phase currents now have 40° displacement (Fig. 15b, bottom plot). Hence, it can be concluded that conversion of the asymmetrical into a symmetrical induction machine was successfully achieved.

V. CONCLUSION

In this paper a general approach for stator winding reconfiguration from symmetrical to asymmetrical (and vice versa), by only rearranging VSI power supply leads in the machine's terminal box, was investigated. The type of the machines where this is possible is identified, and the method for reconfiguration is explained. Winding reconfiguration of a six-phase machine does not conform to the general algorithm. However, because of its importance, a brief discussion is

included. Two (nine- and fifteen-phase) examples of composite odd phase number machines for which this rearrangement is applicable were theoretically studied. By replacing old mimic diagram on the machine with the new one and after rearranging VSI power supply leads accordingly, old nine-phase symmetrical/asymmetrical winding configuration was changed to new asymmetrical/symmetrical one. In addition to the nine-phase, a simplified fifteen-phase machine case was also shown. Based on the examples, a general algorithm for reconfiguration is derived and shown in a flow chart form.

Possible advantages/disadvantages related to winding reconfiguration were also discussed. Theoretical considerations were confirmed experimentally. For this purpose harmonic mapping in a PMSM and parameter identification of an IM, in conjunction with a transient response under FOC, were studied.

REFERENCES

[1] E. Levi, R. Bojoi, F. Profumo, H. A. Toliyat, and S. Williamson, "Multiphase induction motor drives—A technology status review," *IET Electr. Power Appl.*, vol. 1, no. 4, pp. 489–516, Jul. 2007.
[2] M. J. Duran, E. Levi, and F. Barrero, "Multiphase electric drives: Introduction," in *Encyclopedia of Electrical and Electronics Engineering*, J. Webster, Ed. Hoboken, NJ, USA: Wiley, 2017, pp. 1–26.
[3] L. Parsa, "On advantages of multi-phase machines," in *Proc. 31st Ann. Conf. IEEE Ind. Electron. Soc. (IECON)*, Nov. 2005, pp. 1574–1579.
[4] R. Bojoi, F. Farina, F. Profumo, and A. Tenconi, "Dual-three phase induction machine drives control—A survey," *IEEE Trans. Ind. Appl.*, vol. 126, no. 4, pp. 420–429, Jan. 2006.
[5] R. Nelson and P. Krause, "Induction machine analysis for arbitrary displacement between multiple winding sets," *IEEE Trans. Ind. Appl.*, vols. PAS–93, no. 3, pp. 841–848, May 1974.
[6] A. A. Rockhill and T. A. Lipo, "A simplified model of a nine-phase synchronous machine using vector space decomposition," *Electr. Power Compon. Syst.*, vol. 38, no. 4, pp. 477–489, Feb. 2010.
[7] A. A. Rockhill and T. A. Lipo, "A generalized transformation methodology for polyphase electric machines and networks," in *Proc. IEEE Int. Electr. Mach. Drives Conf. (IEMDC)*, May 2015, pp. 27–34.
[8] I. Zoric, M. Jones, and E. Levi, "Arbitrary power sharing among three-phase winding sets of multiphase machines," *IEEE Trans. Ind. Electron.*, vol. 65, no. 2, pp. 1128–1139, Feb. 2018.
[9] R. R. Bastos, R. M. Valle, S. L. Nau, and B. J. C. Filho, "Modelling and analysis of a nine-phase induction motor with third harmonic current injection," in *Proc. 9th Int. Conf. Power Electron. ECCE Asia (ICPE-ECCE Asia)*, Jun. 2015, pp. 688–694.
[10] A. Gautam, S. Karugaba, and J. Ojo, "Modeling of nine-phase interior permanent magnet machines (IPM) including harmonic effects," in *Proc. IEEE Int. Electr. Mach. Drives Conf. (IEMDC)*, May 2011, pp. 681–686.
[11] E. Jung, H. Yoo, S.-K. Sul, H.-S. Choi, and Y.-Y. Choi, "A nine-phase permanent-magnet motor drive system for an ultrahigh-speed elevator," *IEEE Trans. Ind. Appl.*, vol. 48, no. 3, pp. 987–995, May 2012.
[12] F. Li, W. Hua, and M. Cheng, "Design and optimization of a nine-phase flux-switching PM generator for wind power systems," in *Proc. 17th Int. Conf. Electr. Mach. Syst. (ICEMS)*, Oct. 2014, pp. 471–477.
[13] F. Patkar, A. Jidin, E. Levi, and M. Jones, "Performance comparison of symmetrical and asymmetrical six-phase open-end winding drives with carrier-based PWM," in *Proc. 6th Int. Conf. Elect. Eng. Inform. (ICEEI)*, Nov. 2017, pp. 1–6.
[14] E. A. Klingshirn, "High phase order induction motors—Part I-description and theoretical considerations," *IEEE Trans. Power App. Syst.*, vol. PAS-102, no. 1, pp. 47–53, Jan. 1983.
[15] M. Zabaleta, E. Levi, and M. Jones, "A novel synthetic loading method for multiple three-phase winding electric machines," *IEEE Trans. Energy Convers.*, vol. 34, no. 1, pp. 70–78, Mar. 2019.
[16] M. Slunjski, M. Jones, and E. Levi, "Analysis of a symmetrical nine-phase machine with highly non-sinusoidal back-electromotive force," in *Proc. 44th Annu. Conf. IEEE Ind. Electron. Soc.(IECON)*, Oct. 2018, pp. 6229–6234.
[17] A. Cervone, M. Slunjski, E. Levi, and G. Brando, "Optimal third-harmonic current injection for an asymmetrical nine-phase PMSM with non-sinusoidal back-EMF," in *Proc. 45th Annu. Conf. IEEE Ind. Electron. Soc. (IECON)*, Oct. 2019, pp. 6223–6228.
[18] M. Slunjski, M. Jones, and E. Levi, "Control of a symmetrical nine-phase PMSM with highly non-sinusoidal back-electromotive force using third harmonic current injection," in *Proc. 45th Annu. Conf. IEEE Ind. Electron. Soc. (IECON)*, Oct. 2019, pp. 969–974.
[19] A. G. Yepes, J. A. Riveros, J. Doval-Gandoy, F. Barrero, O. Lopez, B. Bogado, M. Jones, and E. Levi, "Parameter identification of multiphase induction machines with distributed windings—Part 1: Sinusoidal excitation methods," *IEEE Trans. Energy Convers.*, vol. 27, no. 4, pp. 1056–1066, Dec. 2012.

MARKO SLUNJSKI (Student Member, IEEE) received the B.Sc. and M.Sc. degrees in electrical engineering from the Faculty of Electrical Engineering and Computing, University of Zagreb, Croatia, in 2015 and 2017, respectively. He is currently pursuing the Ph.D. degree in electrical engineering with Liverpool John Moores University, Liverpool, U.K. Since July 2017, he has been with Liverpool John Moores University. His main research interests are in the areas of power electronics and advanced variable speed multiphase drive systems.

OBRAD DORDEVIC (Member, IEEE) received the Dipl.Ing. degree in electronic engineering from the University of Belgrade, Serbia, in 2008. He joined Liverpool John Moores University, in December 2009, as a Ph.D. student. He received the Ph.D. degree, in April 2013. He was appointed as a Lecturer at Liverpool John Moores University, in May 2013. In 2018, he was promoted to a Reader in power electronics. His main research interests are in the areas of power electronics, electrostatic precipitators, and advanced variable speed multiphase drive systems.

MARTIN JONES received the B.Eng. degree (Hons.) in electrical and electronic engineering and the Ph.D. degree from Liverpool John Moores University, U.K., in 2001. He has been a Research Student with Liverpool John Moores University, from September 2001 to Spring 2005, where he is currently a Reader. He was a recipient of the IEE Robinson Research Scholarship for his Ph.D. studies.

EMIL LEVI (Fellow, IEEE) received the M.Sc. and Ph.D. degrees in electrical engineering from the University of Belgrade, Yugoslavia, in 1986 and 1990, respectively. He joined Liverpool John Moores University, U.K., in May 1992. Since September 2000, he has been a Professor of electric machines and drives. He was a recipient of the Cyril Veinott Award of the IEEE Power and Energy Society, in 2009, and the Best Paper award of the IEEE TRANSACTION ON INDUSTRIAL ELECTRONICS, in 2008. In 2014, he received the Outstanding Achievement Award from the European Power Electronics (EPE) Association and in 2018, the Professor Istvan Nagy Award from the Power Electronics and Motion Control (PEMC) Council. He served as a Co-Editor-in-Chief of the IEEE TRANSACTION ON INDUSTRIAL ELECTRONICS, from 2009 to 2013. He is currently the Editor-in-Chief of the IEEE TRANSACTION ON INDUSTRIAL ELECTRONICS, the Editor-in-Chief of the *IET Electric Power Applications*, and an Editor of the IEEE TRANSACTION ON ENERGY CONVERSION.